

Effects of vector attenuation on AVO of offshore reflections

J. M. Carcione*

ABSTRACT

Waves transmitted at the ocean bottom have the characteristic that, for any incidence angle, the attenuation vector is perpendicular to the ocean-bottom interface (assuming water a lossless medium). Such waves are called inhomogeneous; in this case, the inhomogeneity angle coincides with the propagation angle. The vector character of this transmitted pulse affects the amplitude variation with offset (AVO) response of deeper reflectors. The analysis of the reflection coefficient is performed for a shale (the ocean-bottom sediment) overlying a chalk, assuming no loss in the sea floor and loss with an incident homogeneous wave and an incident inhomogeneous wave. Beyond the elastic critical angle the differences are important, mainly for the incident homogeneous wave. These differences depend not only on the properties of the media but also on the inhomogeneity of the wave.

INTRODUCTION

In offshore seismic exploration, the waves transmitted at the ocean bottom have a particular characteristic. Assuming that water is lossless, their attenuation vectors are perpendicular to the ocean-bottom interface. This fact affects the amplitude variation with offset (AVO) response of reflection events generated at the lower layers.

Winterstein (1987) investigates the general problem from a kinematic point of view. He analyzes how the angle between propagation and maximum attenuation varies in an anelastic layered medium and shows that departures from elastic-wave raypaths can be large. On the other hand, compressional wave reflection coefficients for different incidence inhomogeneity angles are compared by Krebs (1984). He shows that the deviations from the elastic case can be important at supercritical angles.

In this paper I investigate the AVO response for an inhomogeneous wave generated at the ocean bottom and incident at a lower interface separating two viscoelastic transversely isotropic (TI) media. Unlike the analysis performed by Krebs (1984), the inhomogeneity angle is not constant with offset but is equal to the incidence angle, since the interface is assumed to be parallel to the ocean bottom (see Figure 1). The interface may separate two finely layered formations whose contact plane is parallel to the stratification or two media with intrinsic anisotropic properties, such as shale and limestone.

CONSTITUTIVE EQUATIONS

A consistent stress-strain model for anisotropic viscoelasticity is given by Carcione (1995). The convention is to denote with ($\nu = 1$) and ($\nu = 2$) the quasi-dilatational and quasi-shear deformations, respectively. The complex stiffnesses relating stress and strain for a 2-D TI medium can be expressed as

$$p_{11} = c_{11} - \frac{1}{2}(c_{11} + c_{33}) + \left[\frac{1}{2}(c_{11} + c_{33}) - c_{55}\right]M_1 + c_{55}M_2, \quad (1)$$

$$p_{33} = c_{33} - \frac{1}{2}(c_{11} + c_{33}) + \left[\frac{1}{2}(c_{11} + c_{33}) - c_{55}\right]M_1 + c_{55}M_2, \quad (2)$$

$$p_{13} = c_{13} - \frac{1}{2}(c_{11} + c_{33}) + \left[\frac{1}{2}(c_{11} + c_{33}) - c_{55}\right]M_1 + c_{55}(2 - M_2), \quad (3)$$

and

$$p_{55} = c_{55}M_2. \quad (4)$$

The elastic constants c_{IJ} , $I, J = 1, \dots, 6$ are the unrelaxed or high-frequency limit stiffnesses; $M_\nu(\omega)$ are dimensionless complex moduli describing the amount of attenuation. In the purely elastic case ($\omega \rightarrow \infty$) $M_\nu \rightarrow 1$.

Manuscript received by the Editor April 14, 1997; revised manuscript received August 7, 1998.

*Osservatorio Geofisico Sperimentale, P.O. Box 2011 Opicina, 34016 Trieste, Italy. E-mail: jcarcione@ogs.trieste.it.

© 1999 Society of Exploration Geophysicists. All rights reserved.

GENERATION OF INHOMOGENEOUS WAVES

Let us assume that the positive z -axis points downward. A general solution for the particle velocity field $\mathbf{v} = (v_x, v_z)$ is

$$\mathbf{v} = i\omega\mathbf{U} \exp[i\omega(t - s_x x - s_z z)], \quad (5)$$

where s_x and s_z are the components of the complex slowness vector, t is the time variable, and \mathbf{U} is a complex vector. The real slowness vector

$$\mathbf{s}_R \equiv [\text{Re}(s_x), \text{Re}(s_z)]^\top \quad (6)$$

and the attenuation vector

$$\boldsymbol{\alpha} \equiv [\text{Im}(s_x), \text{Im}(s_z)]^\top \quad (7)$$

in general will not point in the same direction; when they do not, waves are called inhomogeneous. Otherwise, the waves are homogeneous, as in 1-D space.

Figure 1 depicts a transmitted inhomogeneous wave generated at the ocean bottom. Since the attenuation vector of waves propagating in the water layer is zero, viscoelastic Snell's law (Wennerberg, 1985) implies that the transmitted attenuation vector is perpendicular to the ocean bottom. Note that the inhomogeneity angle is equal to the propagation angle θ .

The complex slowness relation of a viscoelastic TI medium has the form (e.g., Auld, 1990)

$$\begin{aligned} (p_{11}s_x^2 + p_{55}s_z^2 - \rho)(p_{33}s_x^2 + p_{55}s_z^2 - \rho) \\ - (p_{13} + p_{55})^2 s_x^2 s_z^2 = 0 \end{aligned} \quad (8)$$

and has two solutions, corresponding to the quasi-compressional (qP) and quasi-shear (qS) waves.

The complex slowness components below the ocean bottom are

$$s_x = s_R \sin \theta, \quad s_z = s_R \cos \theta - i \frac{\alpha}{\omega}, \quad (9)$$

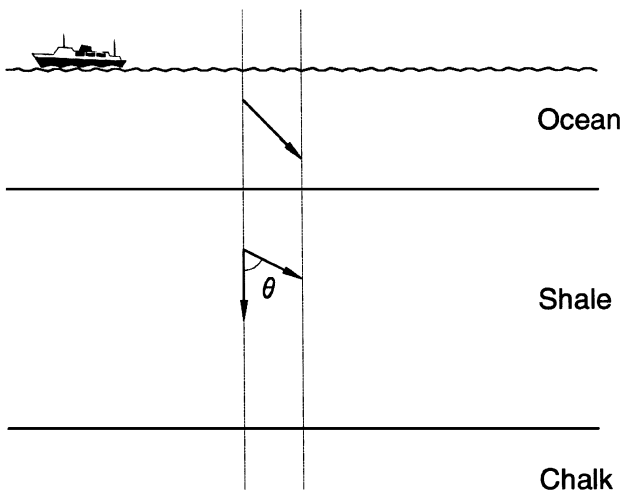


FIG. 1. Snell's law for a plane wave incident on the ocean-bottom interface. The diagram shows the continuity of the horizontal component of the complex slowness vector. In the ocean this vector is real, since water is assumed to be lossless. In the shale layer the attenuation vector is perpendicular to the ocean bottom.

where s_R and α are the magnitudes of \mathbf{s}_R and $\boldsymbol{\alpha}$, respectively. For a given angle θ , s_R and α can be computed from equation (8); substitution of these quantities into equation (9) yields the slowness components of the incident inhomogeneous wave. However, this method requires the numerical solution of two fourth-degree polynomials. A simpler approach is the following.

First, assume a given propagation angle θ_h for a hypothetical transmitted homogeneous wave. Then, the complex slowness is

$$s = \frac{1}{\sqrt{2\rho}} (p_{55} + p_{11} \sin^2 \theta_h + p_{33} \cos^2 \theta_h \pm E)^{-1/2}, \quad (10)$$

where ρ is the density and

$$\begin{aligned} E = \{[(p_{33} - p_{55}) \cos^2 \theta_h - (p_{11} - p_{55}) \sin^2 \theta_h]^2 \\ + (p_{13} + p_{55})^2 \sin^2 2\theta_h\}^{1/2}, \end{aligned} \quad (11)$$

with the plus sign corresponding to the qP -wave and the minus sign to the qS -wave (e.g., Carcione, 1997).

Next, choose s_x for the inhomogeneous wave equal to $\text{Re}(s) \sin \theta_h$ a real quantity (according to Snell's law), since the projection of $\boldsymbol{\alpha}$ on the interface is zero. Then compute s_z from equation (8). Finally, compute the incidence propagation angle θ for the inhomogeneous wave as

$$\theta = \arcsin \left(\frac{s_x}{\sqrt{s_x^2 + [\text{Re}(s_z)]^2}} \right). \quad (12)$$

In this way, a vector (s_x, s_z) , satisfying equation (8) and input to the reflection-transmission problem, can be obtained for each incidence angle θ . The price we pay for this simplicity is that the ray angle does not reach 90° , but this is not important since the offsets of interest in exploration geophysics are sufficiently covered.

REFLECTION-TRANSMISSION PROBLEM

The problem of reflection and refraction at an interface between two TI media whose respective symmetry axes are perpendicular to the interface has been investigated by Graebner (1992) and Carcione (1997) in the elastic and anelastic cases, respectively. He considered a homogeneous incident wave and obtained the attributes of the reflected and transmitted waves such as, for instance, the energy reflection coefficients, the phase and energy velocities, the quality factor, and the interference coefficients.

To distinguish between downward- and upward-propagating waves, the slowness relation (8) is solved for s_z , given the horizontal slowness s_x . It yields

$$s_z = \pm \frac{1}{\sqrt{2}} \left(K_1 \mp p\sqrt{K_1^2 - 4K_2K_3} \right)^{1/2}, \quad (13)$$

where

$$K_1 = \rho \left(\frac{1}{p_{55}} + \frac{1}{p_{33}} \right) + \frac{1}{p_{55}} \left[\frac{p_{13}}{p_{33}} (p_{13} + 2p_{55}) - p_{11} \right] s_x^2,$$

$$K_2 = \frac{1}{p_{33}} (p_{11}s_x^2 - \rho), \quad K_3 = s_x^2 - \frac{\rho}{p_{55}}$$

and $\text{pv}(z)^{1/2}$ denotes the principal value of the square root of the complex number z . The signs corresponds to $(+, -) =$ downward qP -wave, $(+, +) =$ downward qS -wave, $(-, -) =$ upward qP -wave, and $(-, +) =$ upward qS -wave.

Application of welded boundary conditions generates the following matrix equation for the reflection and transmission coefficients R and T :

$$\begin{pmatrix} \beta_{P_1} & \beta_{S_1} & -\beta_{P_2} & -\beta_{S_2} \\ \gamma_{P_1} & \gamma_{S_1} & \gamma_{P_2} & \gamma_{S_2} \\ Z_{P_1} & Z_{S_1} & -Z_{P_2} & -Z_{S_2} \\ W_{P_1} & W_{S_1} & W_{P_2} & W_{S_2} \end{pmatrix} \begin{pmatrix} R_{PP} \\ R_{PS} \\ T_{PP} \\ T_{PS} \end{pmatrix} = \begin{pmatrix} -\beta_{P_1} \\ \gamma_{P_1} \\ -Z_{P_1} \\ W_{P_1} \end{pmatrix}. \tag{14}$$

The upper layer is denoted by the subscript 1 and the lower layer by the subscript 2. The symbols P and S indicate the qP - and qS -waves, respectively. The quantities β and γ are the horizontal and vertical complex polarizations, respectively, given by

$$\beta = \text{pv} \left[\frac{p_{55}s_x^2 + p_{33}s_z^2 - \rho}{p_{11}s_x^2 + p_{33}s_z^2 + p_{55}(s_x^2 + s_z^2) - 2\rho} \right]^{1/2} \tag{15}$$

and

$$\gamma = \pm \text{pv} \left[\frac{p_{11}s_x^2 + p_{55}s_z^2 - \rho}{p_{11}s_x^2 + p_{33}s_z^2 + p_{55}(s_x^2 + s_z^2) - 2\rho} \right]^{1/2}, \tag{16}$$

where the plus and minus signs correspond to the qP - and qS -waves, respectively. Moreover,

$$W = p_{55}(\gamma s_x + \beta s_z) \quad \text{and} \quad Z = \beta p_{13}s_x + \gamma p_{33}s_z, \tag{17}$$

and the ray angle is

$$\tan \psi = \frac{\text{Re}(\beta^* X + \gamma^* W)}{\text{Re}(\beta^* W + \gamma^* Z)}, \tag{18}$$

where

$$X = \beta p_{11}s_x + \gamma p_{13}s_z \tag{19}$$

(Carcione, 1997).

RESULTS AND DISCUSSION

The material properties of the incidence and transmission media (the shale and the chalk, respectively) are given in Table 1, where $V_{IJ} = \sqrt{c_{IJ}/\rho}$. The unrelaxed velocities are indicated in the table, and attenuation is quantified by the parameters $Q_v = \text{Re}(M_v)/\text{Im}(M_v)$. Wright (1987) calculated the reflection coefficients for the elastic case, which is obtained in the unrelaxed limit.

The comparison between the absolute values of the qP -wave reflection coefficients, together with the corresponding phase

Table 1. Material properties.

Rock	V_{11} (m/s)	V_{33} (m/s)	V_{55} (m/s)	V_{13} (m/s)	Q_1	Q_2	ρ (g/cm ³)
Shale	3810	3048	1402	1828	10	5	2.3
Chalk	5029	5029	2621	3414	100	70	2.7

angles, is shown in Figure 2, where E corresponds to the elastic case (i.e., elastic shale), H to an incident viscoelastic homogeneous wave, and I to an incident inhomogeneous wave with the characteristics indicated in Figure 1 (the chalk is assumed anelastic in the three cases). In the purely elastic case, i.e., shale and chalk both elastic (Wright, 1987), there is a critical angle between 40° and 50°. It can be shown that the energy vector of the refracted qP -wave points downward for all incident angles. Thus, there is no critical angle in the strict sense. However, the shape of the E and I curves indicates that a quasi-evanescent wave propagates through the interface. This character is lost in the H curve. In the near-offset (up to 20°), the three coefficients follow the same trend and are very similar each other. The difference with the elastic case (E) is because of the anelastic properties of the shale. Beyond 30° the differences are important, mainly for the incident homogeneous wave. This can also be observed in the phase, where the H curve has the opposite sign with respect to the other curves. A similar effect is reported by Krebes (1984).

Figure 3 represents the energy velocities of the reflected qP -wave for the three cases. The variations with offset are mainly due to shale anisotropy and, as before, the differences with the elastic case (E) are from the anelastic properties of the

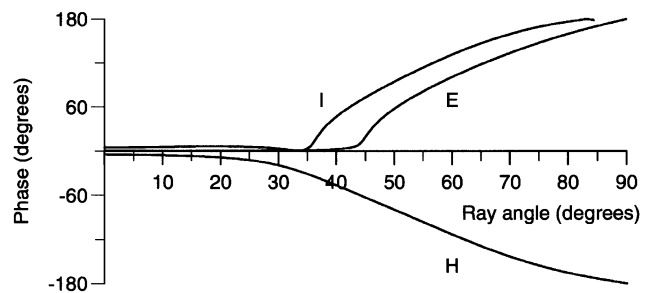
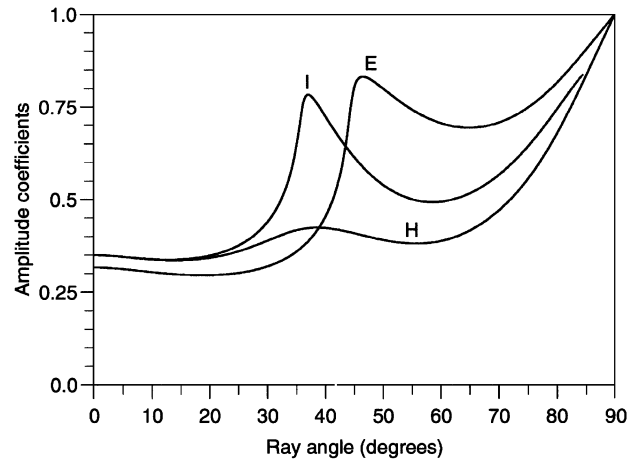


FIG. 2. Comparison between the absolute values of the R_{PP} reflection coefficients together with the corresponding phase angles, where E corresponds to the elastic case (i.e., elastic shale), H to an incident viscoelastic homogeneous wave, and I to an incident inhomogeneous wave with the characteristics indicated in Figure 1.

shale. The elastic velocities are higher than the viscoelastic velocities since the elastic limit corresponds to the high-frequency limit. The attenuation of the reflected qP -wave is shown in Figure 4. For an incident homogeneous wave (H), the variations with angle are solely because of the anisotropic effects. On the contrary, the variations for the (I) curve are attributable to the inhomogeneous character of the wave. It can be shown that a similar trend is obtained for an isotropic shale.

The interference coefficients, displayed in Figure 5, are the result of the interaction of the stress and particle velocity fields of the incident and reflected qP -waves. Much of the energy flow is because of interference beyond the elastic critical angle. For some incident angles, the interference coefficients can have the same magnitude as the reflection coefficients.

To complete the reflection problem, Figures 6–8 show the corresponding curves for the reflected qS -wave resulting from an incident qP -wave. As can be appreciated, mode conversion and anelastic effects are significant beyond the elastic critical angle.

The values of the shale quality factor in Table 1 correspond to a very unconsolidated sea-floor sediment. Typical values for marine sediments can be found in Hamilton (1972), with compressional quality factors of approximately 30 (S -wave quality factors are not reported). Let us consider $Q_1 = 30$ and $Q_2 = 10$, which are close to the values measured by McDonal et al.

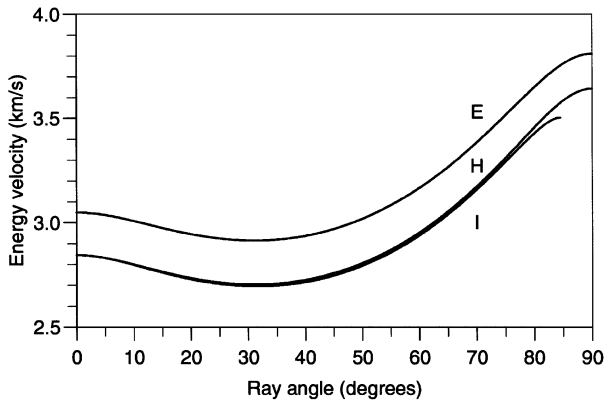


FIG. 3. Comparison between the energy velocities of the reflected qP -wave for the three cases indicated in Figure 2.

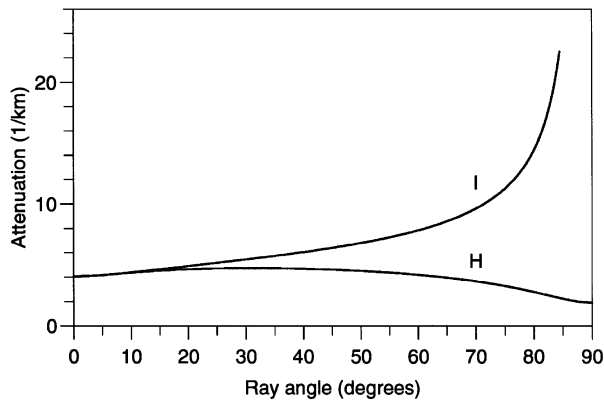


FIG. 4. Comparison between the attenuation magnitudes of the reflected qP -wave for the three cases indicated in Figure 2.

(1958) in Pierre Shale. Figure 9 compares the absolute values of the qP -wave reflection coefficients and the corresponding phase angles for the three cases illustrated in Figure 2. As can be appreciated, the differences are still important, mainly at supercritical angles.

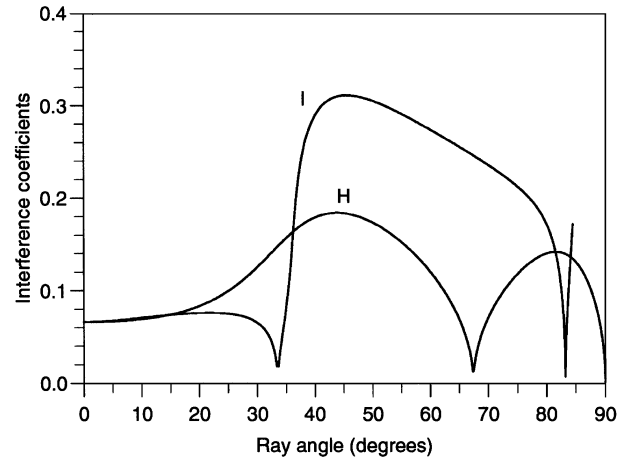


FIG. 5. Comparison between the interference coefficients of the incident homogeneous (H) and inhomogeneous (I) waves. The coefficients correspond to the interaction of the stress and particle velocity fields of the incident and reflected qP -waves.

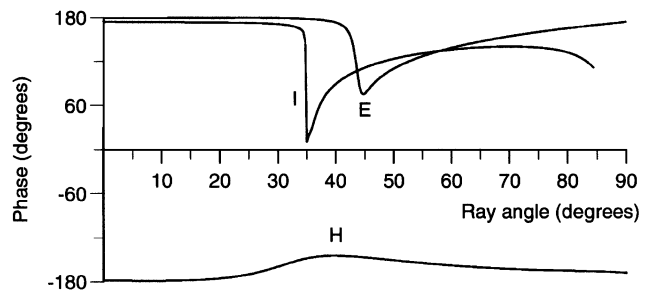
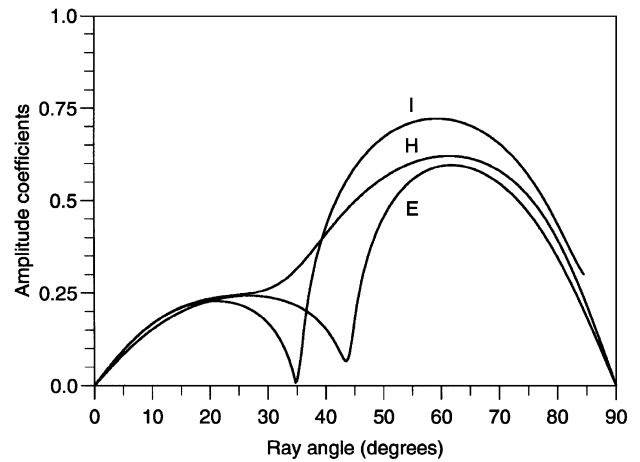


FIG. 6. Comparison between the absolute values of the R_{PS} reflection coefficients together with the corresponding phase angles. The different cases are indicated in Figure 2.

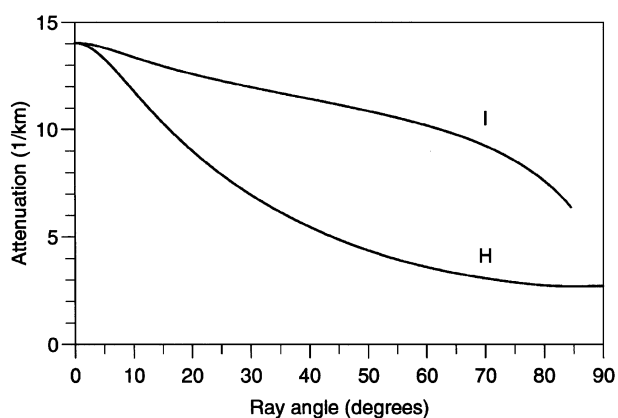


FIG. 7. Comparison between the attenuation magnitudes of the reflected qS -wave as the result of an incident qP -wave. The different cases are indicated in Figure 2.

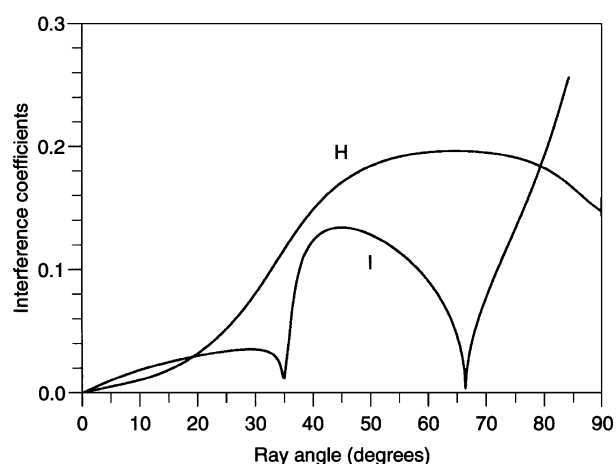


FIG. 8. Comparison between the interference coefficients for incident homogeneous (H) and inhomogeneous (I) waves. The coefficients correspond to the interaction of the stress and particle velocity fields of the incident qP -wave and reflected qS -wave.

CONCLUSIONS

AVO studies in the presence of a highly attenuating ocean bottom (e.g., unconsolidated sediments) should not be based on forward models and processing techniques that assume simplified rheologies or neglect the vector attenuation character of the seismic pulse. These properties affect not only the analysis of the shallow layers but also the inversion of the deeper reflectors.

Amplitude and phase differences are significant at supercritical angles. Variations of the attenuation depend on both the anisotropic properties and the inhomogeneity of the wave. Moreover, for certain offsets, energy flows produced by interference of stress and particle velocity can be comparable to the energy flux of the reflected waves, an effect that does not occur in perfect elasticity.

The analysis does not take into account the amplitude variations with angle of the incident inhomogeneous wave generated at the ocean bottom. This is an additional effect to consider in the AVO inversion process.

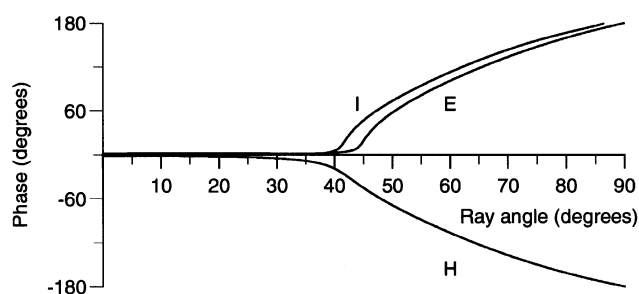
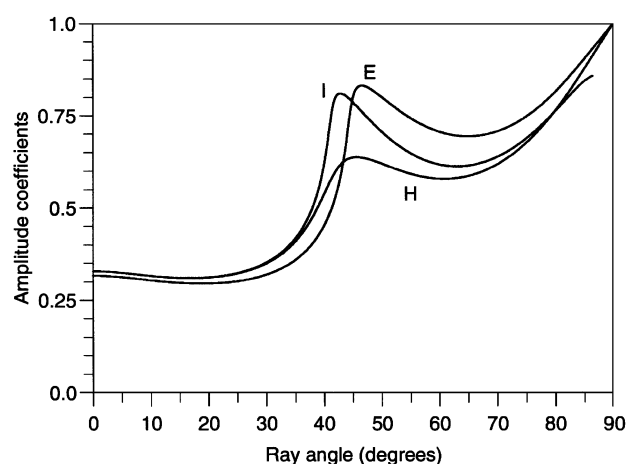


FIG. 9. Comparison of the absolute values of the R_{PP} reflection coefficients and the corresponding phase angles for the three cases indicated in Figure 2, with a sea-floor attenuation defined by $Q_1 = 30$ and $Q_2 = 10$.

ACKNOWLEDGMENTS

I thank the Source Rock project (Norsk Hydro) for financing the research.

REFERENCES

- Auld, B. A., 1990, Acoustic fields and waves in solids, 1: Robert E. Krieger, Publ. Co.
- Carcione, J. M., 1995, Constitutive model and wave equations for linear, viscoelastic, anisotropic media: *Geophysics*, **60**, 537–548.
- , 1997, Reflection and refraction of qP - qS plane waves at a plane boundary between viscoelastic transversely isotropic media: *Geophys. J. Internat.*, **129**, 669–680.
- Graebner, M., 1992, Plane-wave reflection and transmission coefficients for a transversely isotropic solid: *Geophysics*, **57**, 1512–1519.
- Hamilton, E., 1972, Compressional wave attenuation in marine sediments: *Geophysics*, **37**, 620–646.
- Krebs, E. S., 1984, On the reflection and transmission of viscoelastic waves—Some numerical results: *Geophysics*, **49**, 1374–1380.
- McDonal, F. J., Angona, F. A., Mills, R. L., Sengbush, R. L., Van Nostrand, R. G., and White, J. E., 1958, Attenuation of shear and compressional waves in Pierre shale: *Geophysics*, **23**, 421–439.
- Wennerberg, L., 1985, Snell's law for viscoelastic materials, *Geophys. J. Roy. Astr. Soc.*, **81**, 13–18.
- Winterstein, D. F., 1987, Vector attenuation: Some implications for plane waves in anelastic layered media: *Geophysics*, **52**, 810–814.
- Wright, J., 1987, The effects of transverse isotropy on reflection amplitude versus offset: *Geophysics*, **52**, 564–567.